Article ID: 1000-324X(2017)03-0326-05 **DOI:** 10.15541/jim20160332

Growth, Magnetic and Electrical Transport Properties of $La_{0.7}Sr_{0.3}MnO_3$ Thin Films on PLZST Ceramics

XIAO Ling[1], CHEN Ying[1], LIU Zhen[1], WANG Gen-Shui[1], WEN Zhi-Yu[2], DONG Xian-Lin[1]

(1. CAS Key Lab of Inorganic Functional Materials and Devices, Shanghai Institute of Ceramics, Chinese Academy of Sciences, Shanghai 200050, China; 2. Micro-system Center, Chongqing University, Chongqing 400030, China)

Abstract: $La_{0.7}Sr_{0.3}MnO_3$ (LSMO) thin films with different thicknesses were deposited on $(Pb_{0.97}La_{0.02})(Zr_{0.58}Sn_{0.3025}Ti_{0.1175})O_3$ (PLZST) ceramics by RF magnetron sputtering, and their microstructure, magnetic and electrical transport properties were investigated. Microscopy observations show that LSMO thin films are perovskite structure without obvious impurity phase. All the LSMO thin films display smooth surface with uniform, and roughness is as low as 2.93 nm for LSMO thin films at the thickness of 20 nm. Furthermore, large magnetoresistance (MR) effect was observed in LSMO thin films in a broad temperature range of 10–300 K. Particularly the MR of LSMO thin films with 20 nm in thickness exhibits excellent temperature stability. Moreover, the Curie temperature, metal-insulator transition temperature, saturation magnetization and electrical conductivity decrease as the film thickness increases, which is attributed to the diffusion of Pb, Sn, Zr, *etc*. in the samples, resulting in the distortion of MnO_6 octahedron.

Key words: $La_{0.7}Sr_{0.3}MnO_3$ thin films; PLZST ceramics; magnetoresistance; diffusion

$La_{1-x}Sr_xMnO_3$ (LSMO) have been extensively investigated in the past decades due to their tantalizing transport properties, such as colossal magnetoresistance (CMR) and half-metallicity[1-2], which make them very promising candidates for applications in future generation microelectronic devices, including magnetic field sensors, transducers, hard disk heads, *etc*[3-5]. The magnetic and electrical transport properties of LSMO films are known to be very sensitive to the nature of substrates, because of the strains imposed by the lattice mismatch and thermal expansion between the film and substrate. For example, strain induced by substrate can suppresses ferromagnetism and reduces the ferromagnetic Curie temperature due to strain-induced distortion of MnO_6 octahedron[6]. In addition, the substrate-induced stress may lead to the structural disorder or defect, which greatly influence the electrical transport properties of films[7].

Recently, extensive studies have been focused on LSMO thin films grown on single crystal substrates ($SrTiO_3$, $LaAlO_3$, $DyScO_3$, Si, *etc*[8-11]). However, no research regarding LSMO thin films deposited on perovskite ceramics is reported. Lanthanum doped lead zirconate stannate titanate (PLZST) ceramics, with perovskite structure, have been widely explored due to their multiple phase transition behaviors and various external field induced properties[12-13]. Up to now, there is no report on PLZST ceramic acting as substrate. In fact, the perovskite structure and lattice constant of PLZST can match well with LSMO. In addition, the PLZST ceramics are cheap and can be made in large size compared with the single crystal substrates, such as $DyScO_3$, $SrTiO_3$. So the PLZST ceramics can be expected to be good substrates for the growth of LSMO thin films. In this paper, LSMO thin films were grown on PLZST ceramics by RF magnetron sputtering, and their magnetic and electrical transport properties were investigated.

1 Experimental

$La_{0.7}Sr_{0.3}MnO_3$ (LSMO) thin films were deposited on $(Pb_{0.97}La_{0.02})(Zr_{0.58}Sn_{0.3025}Ti_{0.1175})O_3$ (PLZST) ceramics by RF magnetron sputtering. The fabrication process of the PLZST ceramics can be found elsewhere[12]. Here, PLZST ceramics were polished and then cleaned. Root roughness

Received date: 2016-05-24; **Modified date:** 2016-07-10
Foundation item: National Natural Science Foundation of China (51302295, 61371059); Natural Science Foundation of Shanghai (13ZR1445600); Visiting Scholar Foundation of Key Discipline Laboratory of New Micro/Nano Device and System Technology in Chongqing University (2014MS05)
Biography: XIAO Lin(1990–), female, candidate of Master degree. E-mail: 13916314676@163.com
Corresponding author: DONG Xian-Lin, professor. E-mail: xldong@mail.sic.ac.cn

mean square (RMS) roughness of the surface of PLZST was ~ 2 nm. The deposition was carried out in an argon-oxygen flow with 80% Ar and 20% O_2, at a pressure of 1 Pa, and a substrate temperature of 500℃. After deposition, the films were post-annealed at 750℃ for 30 min in air and cooled to room temperature naturally. Films with different thicknesses were obtained by changing the deposition time. The thicknesses of films were measured to be 20 nm, 65 nm and 120 nm using scanning electron microscope (SEM, Magellen-2000). The surface morphology of LSMO thin films were obtained using an atomic force microscopy (AFM, Nanonavi probe station, SII, Japan). The phase structures were characterized by X-ray diffraction (XRD, D/max-2550V, Rigaku, Japan). Physical Property Measurement System (PPMS-9, Quantum Design, USA) was used for the measurement of the magnetic and electrical transport properties.

2 Results and Discussion

Figure 1 shows the standard XRD patterns of LSMO thin films with different thicknesses deposited on PLZST ceramics. As shown in the XRD patterns, all the diffraction peaks can be perfectly indexed to the perovskite structure. The intensity of LSMO thin films peaks is weaker than those of PLZST substrate, which may be ascribed to their different thicknesses (0.5 mm for PLZST substrate). The inset of Fig. 1 depicts an enlarged view of the (110) reflections of the LSMO thin films. As the thicknesses increase, the (110) peak of LSMO thin films moves to lower angle at first, and then shifts to higher angle, it means that the lattice constant of LSMO firstly increases and then decreases with thickness increase.

Figure 2 presents the topography images of LSMO thin films. All the films display smooth surface and the root

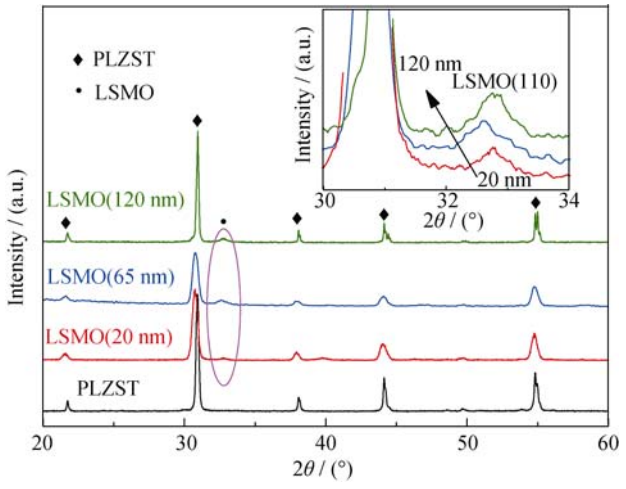

Fig. 1　XRD patterns of LSMO thin films with different thicknesses

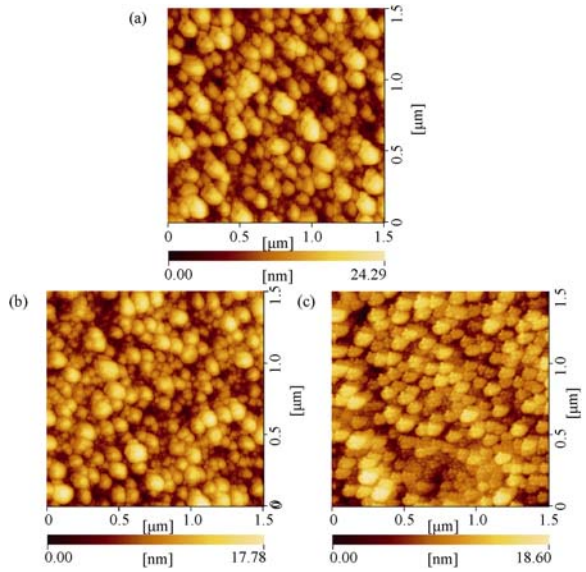

Fig. 2　AFM surface morphologies of LSMO thin films with different thicknessess
(a) 120 nm; (b) 65 nm; (c) 20 nm

mean square (RMS) roughness was characterized to be 4.13 nm, 2.98 nm and 2.93 nm for 120 nm, 65 nm and 20 nm films, respectively. The films tend to be smoother with the decrease of thickness. There is no obvious variation in average grain size detected for those films. However, the grain sizes of 20 nm films are distributed more uniformly compared to the thin films with 65 nm and 120 nm in thickness.

To understand the interaction of LSMO film and PLZST substrate, the interfacial properties of LSMO thin films on PLZST were studied. The cross section SEM images and the energy dispersive spectroscopy (EDS) line scanning along the thickness direction, from the surface of LSMO thin films to PLZST substrate, is shown in Fig. 3. Evident diffusion behaviors between LSMO and PLZST were observed. Moreover, the diffusion amounts of Pb, Zr, and Sn in LSMO films increase as the thicknesses increase. In this work, the temperature of PLZST ceramic substrates was 500℃ all the time during the deposition of LSMO thin films. At this temperature, the diffusion of Pb, Sn, Zr, *etc*. happened. So with the increase of deposition time, both the thicknesses of films and the diffusions are increased.

Pb^{2+} can be accommodated in the La (Sr) site of the perovskite lattice, and Sn^{4+}, Zr^{4+} in the Mn site. The radius of Pb^{2+} is larger than La^{3+} and Sr^{2+} (r_{La}^{3+}=0.136 nm, r_{Sr}^{2+}= 0.1244 nm, r_{Pb}^{2+}= 0.149 nm), the radii of Sn^{4+} and Zr^{4+} are also bigger than Mn^{4+} (r_{Mn}^{4+}=0.053 nm, r_{Sn}^{4+}=0.069 nm, r_{Zr}^{4+}=0.078 nm)[14]. Therefore, the substitution of Mn or Sr (La) by Zr (Sn) or Pb can cause the increment of lattice constant of LSMO thin films[15-16]. With the continuous increase of diffusion, the second phases such as PbO, ZrO_2

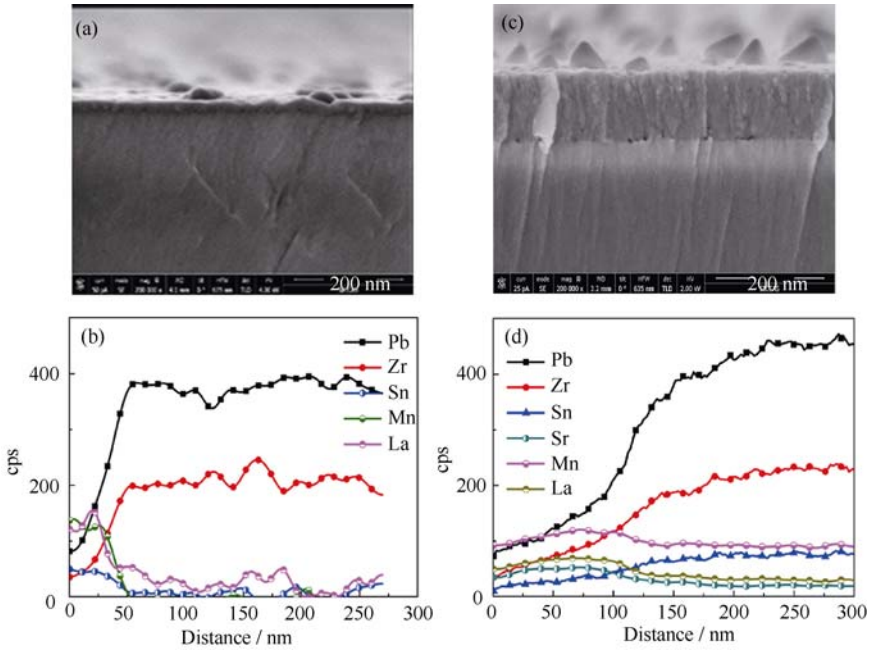

Fig. 3 Cross section SEM and energy dispersive spectroscopy line profiles of LSMO thin films
(a, b) 20 nm; (c, d) 120 nm

and SnO_2 may emerge, and locate at the grain boundaries serving as barrier, which result in the decrease of lattice constant of films. The analysis above is consistent with the variation of lattice constant demonstrated from the XRD patterns.

Fig. 4(a) shows the temperature dependence of resistivity of LSMO with different thicknesses under zero field. Increment in resistivity and decline in metal-insulator transition temperature (T_{MI}) are observed with the increase of thickness. The T_{MI} are 265 K, 255 K, 250 K for LSMO thin films with 20 nm, 65 nm and 120 nm in thickness, respectively. The diffusion of Pb, Zr, Sn in LSMO thin films leads to random local lattice distortion by causing the random displacement of oxygen ions, thereby resulting in the distortion and rotation of MnO_6 octahedron and hence the strong charge carrier localization[17], which should be responsible to the increase of resistivity as the thickness increases.

Fig. 4(b) displays magnetoresistance (MR) values as a function of temperature under applied magnetic field of 6 T. The MR is defined as MR=(R(0)–R(H))/R(0)×100%, where R(H) and R(0) represent the resistivity measured with and without applied magnetic field, respectively. Large MR effect was observed in all samples in the temperature range from 10 K to 300 K, and the MR increase slightly with increasing thickness. The largest MR value reaches 38% in 120 nm films at 10 K. The enhancement of MR with increasing thickness can be attributed to grain tunneling effect due to the increased structural disorder and defects which were caused by the substitution of Mn and La (Sr) in LSMO[18]. Moreover, the MR value of LSMO films at the thickness of 20 nm exhibits excellent temperature stability in the temperature range from 10 K to 250 K, which can be ascribed to the more uniform grain size and less diffusion than the films with 65 nm

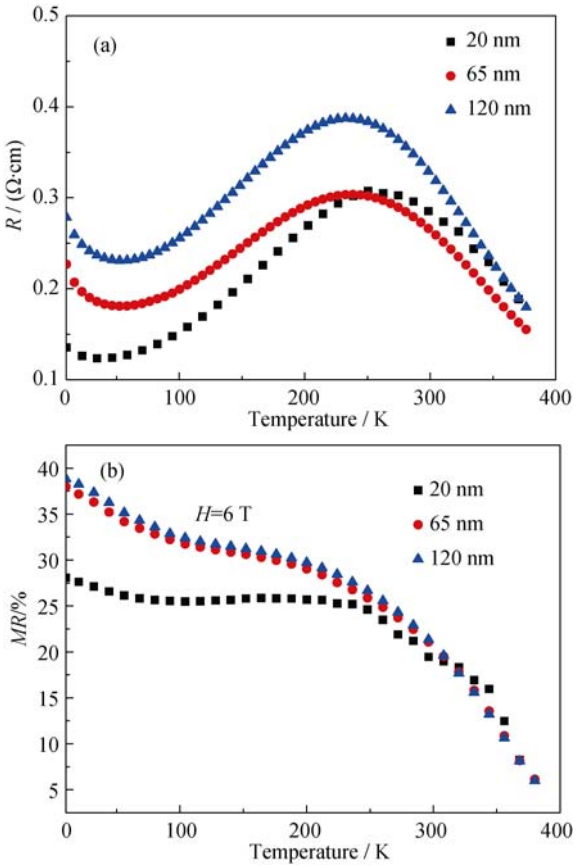

Fig. 4 Temperature dependent resistivity of LSMO films under zero field (a) and temperature-dependent magnetoresistance of LSMO films under 6 T (b)

and 120 nm in thickness.

The low field magnetoresistance (LFMR) properties of LSMO were measured at 250 K and presented in Fig. 5. When the applied field H is scanned from -5 kOe to 5 kOe and back, the LFMR properties become much more obvious with the increase of thickness. Two sharp peaks at low fields (about 800 Oe) were observed in LSMO films with 120 nm in thickness, when the thickness drop to 65 nm, the peaks become broad and finally disappear for 20 nm films. The enhancement of LFMR effect can be attributed to the increase of the structural disorder and defects in thicker LSMO films. It will make the strong spin-dependent scattering of transport electrons at grain boundaries[19-20].

Fig. 6(a) presents the magnetization as a function of temperature in zero-field-cooled (ZFC) processes for theLSMO films with different thicknesses. All of the samples exhibit typical ferromagnetic-paramagnetic transition behavior. The Curie temperature (T_C) of LSMO thin films of 120 nm is nearly 300 K, while the T_C increases to ~340 K for 20 nm films, according to the temperature dependence of the derivative of magnetization shown in the inset of Fig. 6(a). Meanwhile, the ferromagnetic-paramagnetic transition zone becomes sharp with decreasing thickness.

Figure 6(b) presents the magnetic hysteresis loops of LSMO thin films with different thickness measured at 300 K. Increases of saturation magnetization with decreasing thickness were observed, which may be derived from the interaction between LSMO films and PLZST substrates.

The magnetic properties of LSMO have traditionally been examined within the framework of "Double Exchange (DE)", which considers the magnetic coupling between spin aligned Mn^{3+} and Mn^{4+} ions through oxygen sites[21]. The substitution of Mn by Zr (Sn) in LSMO thin films causes a significant decrease in the ferromagnetic ordering compared to un-doped system[22]. Zr^{4+} and Sn^{4+} are non-magnetic ions and do not possess any unpaired electrons. Thus the substitution of Mn by Zr and Sn produces a sudden break in the ferromagnetic Mn^{3+}-O-Mn^{4+} interactions and then leads to the decrease of T_C and magnetization because of magnetic dilution.

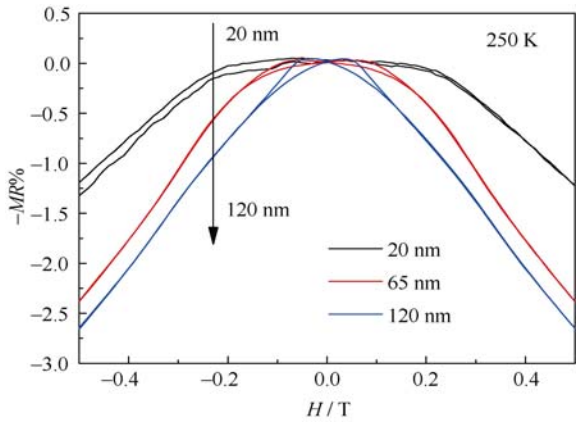

Fig. 5　Magnetic field dependence of MR ratio of LSMO films with different thicknesses at 250 K

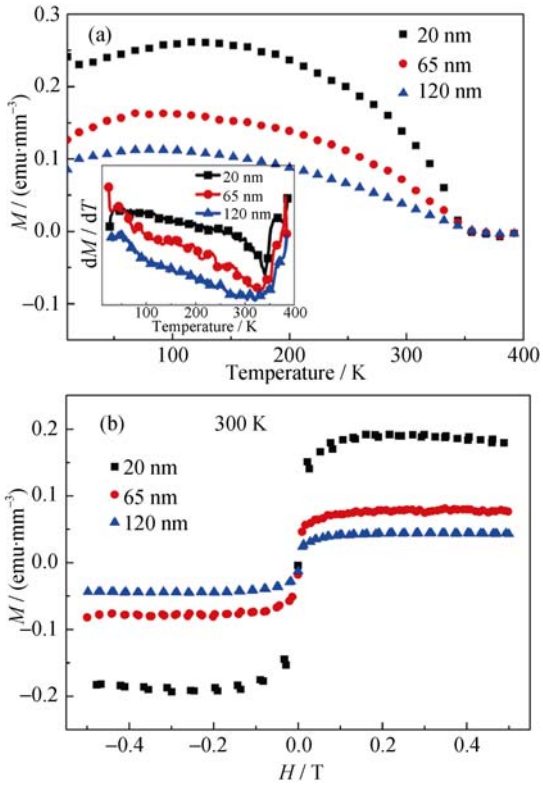

Fig. 6　(a) Temperature dependence of magnetization of LSMO thin films with inset showing temperature dependence of the derivative of magnetization and (b) magnetic hysteresis loops of LSMO thin films with different thicknesses measured at 300 K

3　Conclusions

In summary, LSMO thin films were successefully deposited on PLZST ceramics through RF magnetron sputtering, and their microstructure, magnetic properties and transport properties were investigated. The AFM images show that the LSMO films of 20 nm displays more uniform grain size distribution and the RMS roughness is as low as 2.93 nm. Meanwhile, large MR effect was observed in LSMO films in the temperature range from 10 K to 300 K. Particularly the MR of LSMO films with 20 nm in thickness exhibits excellent temperature stability. The magnetoresistance (MR) ratio increase slightly with the increase of thickness, which can be ascribed to spin-dependent tunneling effect resulted from the enhanced structural disorder. Moreover, the T_C, M_S, T_{MI} and electrical conductivity all decrease as the thickness increases, which can be attributed to the distortion of MnO_6 octahedron arising from the diffusion of Pb, Sn, Zr in LSMO films.

References:

[1] PARK J H, VESCOVO E, KIM H J, *et al.* Direct evidence for a half-metallic ferromagnet. *Nature*, 1998, **392(6678):** 794–796.

[2] HAGHIRT-GOSNET. A M, RENARD J P. CMR manganites: physics, thin films and devices. *J. Phys. D Appl. Phys.*, 2003, **36(8):** 127–150.

[3] CAVALLINI M, GRAZIOSI P, CALBUCCI M, *et al.* Selective electrochemical decomposition of outgrowths and nanopatterning in $La_{0.7}Sr_{0.3}MnO_3$ perovskite thin films. *Scientific Reports*, 2014, **4:** 7397.

[4] JOSHI A, NORI R, DHOBALE S, *et al.* Grain boundary engineering of $La_{0.7}Sr_{0.3}MnO_3$ films on silicon substrate: scanning tunneling microscopy-spectroscopy study. *Physica B: Condensed Matter*, 2014, **448:** 85–89.

[5] XU Z, YU L, WU Y, *et al.* Low-energy resistive random access memory devices with no need for a compliance current. *Scientific Reports*, 2015, **5:** 10409.

[6] MILLIS A J, DARLING T, MIGLIORI A. Quantifying strain dependence in "colossal" magnetoresistance manganites. *Journal of Applied Physics*, 1998, **83(3):** 1588–1591.

[7] MAJUMDAR S, HUHTINEN H, PATURI P, *et al.* Effect of strain and grain boundaries on dielectric properties in $La_{0.7}Sr_{0.3}MnO_3$ thin films. *Journal of Materials Science*, 2012, **48(5):** 2115–2122.

[8] WAHLER M, BÜTTNER B, BLASCHEK H H, *et al.* Controlling magnetic anisotropy in $La_{0.7}Sr_{0.3}MnO_3$ nanostructures. *Applied Physics Letters*, 2014, **104(5):** 052408.

[9] YIN X, MAJIDI M A, CHI X, *et al.* Unraveling how electronic and spin structures control macroscopic properties of manganite ultra-thin films. *NPG Asia Materials*, 2015, **7(7):** e196.

[10] WANG B, YOU L, REN P, *et al.* Oxygen-driven anisotropic transport in ultra-thin manganite films. *Nature Communications*, 2013, **4:** 2778.

[11] CHEN YING, ZHANG SHUAI, DONG XIANLIN, *et al.* Preparation and characterization of lanthanum strontium manganite thin films by metal-organic chemical liquid deposition. *Journal of the American Ceramic Society*, 2011, **94(9):** 2783–2787.

[12] LIU Z, CHEN X, PENG W, *et al.* Temperature-dependent stability of energy storage properties of $Pb_{0.97}La_{0.02}(Zr_{0.58}Sn_{0.335}Ti_{0.085})O_3$ antiferroelectric ceramics for pulse power capacitors. *Applied Physics Letters*, 2015, **106(26):** 262901.

[13] HAO X, ZHAI J, KONG L B, *et al.* A comprehensive review on the progress of lead zirconate-based antiferroelectric materials. *Progress in Materials Science*, 2014, **63:** 1–57.

[14] SHANNON R D. Revised effective ionic radii and systematics. *Acta Cryst.*, 1976, **A32:** 751–767.

[15] RANA D S, THAKER C M, MAVANI K R, *et al*. Magnetic and transport properties of $(La_{0.7-2x}Eu_x)(Ca_{0.3}Sr_x)MnO_3$: effect of simultaneous size disorder and carrier density. *Journal of Applied Physics*, 2004, **95(9):** 4934.

[16] KAMELI P, SALAMATI H, ESHRAGHI M, *et al*. The effect of TiO_2 doping on the structure and magnetic and magneto-transport properties of $La_{0.75}Sr_{0.25}MnO_3$ composite. *Journal of Applied Physics*, 2005, **98(4):** 043908.

[17] ESHRAGHI M, SALAMATI H, KAMELI P. The effect of NiO doping on the structure, magnetic and magnetotransport properties of $La_{0.8}Sr_{0.2}MnO_3$ composite. *Journal of Alloys and Compounds*, 2007, **437(12):** 22–26.

[18] RODRIGUEZ-MARTINEZ L M, ATTFIELD J PAUL. Cation disorder and the metal-insulator transition temperature in manganese oxide perovskites. *Physical Review B*, 1998, **58:** 2426–2429.

[19] HWANG H Y, CHEONG S W, ONG N P, *et al.* Spin-polarized intergrain tunneling in $La_{2/3}Sr_{1/3}MnO_3$. *Physical Review Letter*, 1996, **77(10):** 2041–2044.

[20] GUPTA A, GONG G Q, XIAO G. Grain-boundary effects on the magnetoresistance properties of perovskite manganite films. *Physical Review B*, 1996, **54(22):** 629–632.

[21] ZENER C. Interaction between thed-Shells in the transition metals. II. Ferromagnetic compounds of manganese with perovskite structure. *Physical Review*, 1951, **82(3):** 403–405.

[22] ARAYEDH B, KALLEL S, KALLEL N, *et al*. Influence of non-magnetic and magnetic ions on the MagnetoCaloric properties of $La_{0.7}Sr_{0.3}Mn_{0.9}M_{0.1}O_3$ doped in the Mn sites by M=Cr, Sn, Ti. *Journal of Magnetism and Magnetic Materials*, 2014, **361:** 68–73.

PLZST 陶瓷衬底上 $La_{0.7}Sr_{0.3}MnO_3$ 薄膜生长及其磁性能和电输运特性研究

肖 玲[1], 陈 莹[1], 刘 振[1], 王根水[1], 温志渝[2], 董显林[1]

(1. 中国科学院 上海硅酸盐研究所, 无机功能材料与器件重点实验室, 上海 200050; 2. 重庆大学 微系统中心, 重庆 400044)

摘 要: 采用磁控溅射法在 PLZST 陶瓷衬底上制备了不同厚度的 LSMO 薄膜, 并对其微结构、磁性能及电输运特性进行了研究。结果表明, LSMO 薄膜具有单一钙钛矿结构, 晶粒均匀, 表面平整, 其中 20 nm 厚 LSMO 薄膜粗糙度仅为 2.93 nm。在 10~300 K 温度范围内, LSMO 薄膜均具有大的磁电阻效应, 20 nm 厚的 LSMO 薄膜磁电阻温度稳定性优异。随着薄膜厚度的增加, 薄膜的居里温度、金属绝缘体转变温度、磁化强度和导电性能降低。这可能是由于 Pb、Sn、Zr 等离子扩散进入 LSMO 薄膜中, 导致 MnO_6 八面体畸变造成的。

关 键 词: LSMO 薄膜; PLZST 陶瓷; 磁电阻; 扩散

中图分类号: TQ174 **文献标识码:** A